ACS APPLIED MATERIALS & INTERFACES

Research Article

www.acsami.org

Tracking the Effect of Adatom Electronegativity on Systematically Modified AlGaN/GaN Schottky Interfaces

Maria Reiner,*[,†,‡] Rudolf Pietschnig,[‡] and Clemens Ostermaier[†]

[†]Infineon Technologies Austria AG, Siemensstr. 2-5, 9500 Villach, Austria

[‡]Institute of Chemistry and CINSaT, University of Kassel, Heinrich-Plett-Str. 40, 34132 Kassel, Germany

ABSTRACT: The influence of surface modifications on the Schottky barrier height for gallium nitride semiconductor devices is frequently underestimated or neglected in investigations thereof. We show that a strong dependency of Schottky barrier heights for nickel/aluminum−gallium nitride (0001) contacts on the surface terminations exists: a linear correlation of increasing barrier height with increasing electronegativity of superficial adatoms is observed. The negatively charged adatoms compete with the present nitrogen over the available gallium (or aluminum) orbital to form an electrically improved surface termination. The resulting modification of the surface dipoles and hence polarization of the surface termination causes observed band bending. Our findings suggest that the greatest Schottky barrier heights are achieved by increasing the concentration of the most polarized fluorine−gallium (−aluminum) bonds at the surface. An increase in barrier height from 0.7 to 1.1 eV after a 15% fluorine termination is obtained with ideality factors of 1.10 ± 0.05. The presence of surface dipoles that are changing the surface energy is proven by the sessile drop method as the electronegativity difference and polarization influences the contact angle. The extracted decrease in the Lifshitz−van-der-Waals component from 48.8 to 40.4 mJ/m^2 with increasing electronegativity and concentration of surface adatoms confirms the presence of increasing surface dipoles: as the polarizability of equally charged anions decreases with increasing electronegativity, the diiodomethane contact angles increase significantly from 14° up to 39° after the 15% fluorine termination. Therefore, a linear correlation between increasing anion electronegativity of the (Al)GaN termination and total surface energy within a 95% confidence interval is obtained. Furthermore, our results reveal a generally strong Lewis basicity of (Al)GaN surfaces explaining the high chemical inertness of the surfaces.

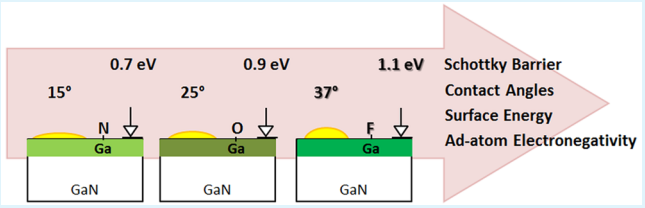

KEYWORDS: *AlGaN, surfaces modification, Schottky barrier height, contact angle, surface energy, adatoms, interface dipole*

INTRODUCTION

Gallium nitride (GaN) represents a promising wide bandgap material[1] for several high-power devices with fast switching behavior, such as high electron mobility transistors (HEMTs)[2] and heterojunction diodes. Due to their fast switching performance rectifying metal−semiconductor Schottky contacts are the typical choice for the gate. The potential energy difference between the semiconductor electron affinity and the metal work function that is seen by the carriers during electronic transport is called Schottky barrier height (Φ_{SB}).[3] Large and stable Φ_{SB} values are often preferred causing an increase in threshold voltage for HEMTs and a reduction in Schottky leakage currents.

Several physical mechanisms[4] are known to determine the height of the Schottky barrier. For ideal, hence abrupt, homogeneous, and defect-free rectifying metal−semiconductor junctions, the theoretic Mott−Schottky model applies, where the barrier height is given as the difference of semiconductor electron affinity and metal work function. However, for nickel (Ni) on GaN contacts, the surface barrier is reported to vary between 0.56 and 1.09 eV.[5] This is because real barrier heights may be influenced by the presence of interface states that are formed due to adatoms or interface structures.[6] The presence of heterogeneous adatoms can cause the formation of adsorption-induced surface dipoles:[7] as the dipole indicates the direction of electronic charge transfer, it will increase or decrease the Φ_{SB} dependent on an increased or decreased electronegativity differences between the semiconductor and the adatom[8] respectively.

Surface dipole changes are known to influence the general wetting behavior of a solid−liquid−gas system.[9] At the equilibrium of such a wetting system, the Gibbs energy is at its minimum and Young's equation applies; thus the cosine of the contact angle (θ) of a droplet on a solid relates to the surface tension. Solely the termination of a solid, hence its 1−3 top atomic layers, are proposed to determine the free surface energy.[10] Adsorption of atoms that lead to surface modifications will influence the wetting behavior and therefore the free surface energy of the GaN surface. The presence of increased amounts of surface dipoles will increase the interaction with polar solvents. $Al_xGa_{1-x}N$ is found to have an improved wetting behavior over GaN with increasing Al content (x) in $Al_xGa_{1-x}N$.[11] This may be explained by an increased amount

Received: July 29, 2015
Accepted: October 5, 2015
Published: October 5, 2015

DOI: 10.1021/acsami.5b06918
ACS Appl. Mater. Interfaces 2015, 7, 23124−23131

Scheme 1. Schematic Illustration of Increased Ni/AlGaN Schottky Barrier Heights (eV) and Increasing Diiodomethane Contact Angles (deg) on $Al_xGa_{1-x}N$ Surfaces (x = 0.22) Due to Increasing Electronegativity of the Surface Termination: Nitride Rich (or Low Carbon and Oxygen) over Oxygen Rich to Fluorine Rich Surfaces[a]

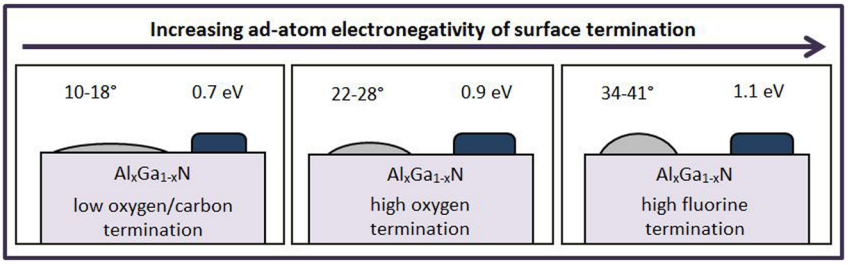

[a]The deviation is due to a relative failure of 2−3° during contact angle measurements and surface atom concentrations; however, as there are no overlying values, a systematic increase can clearly be obtained.

Table 1. Process Parameters for Processes A−G on GaN and AlGaN Surfaces

process	A	B	C	D	E	F	G
media	ref	$HCl/H_2O_2/H_2O$ (1:1:2)	3% HF/H_2O	$BCl_3/Cl_2/O_2$ plasma	O_2 plasma	CF_4/O_2 plasma	NF_3/N_2 plasma
time [min]	na	15	10	1	1.5	1.5	1.5
temp [°C]	na	60	25	60	300	65	65
other	storage	N_2 dry	N_2 dry	13 mTorr, 200 W	0.7 Torr, 700 W	0.9 Torr, 800 W	0.9 Torr, 800 W

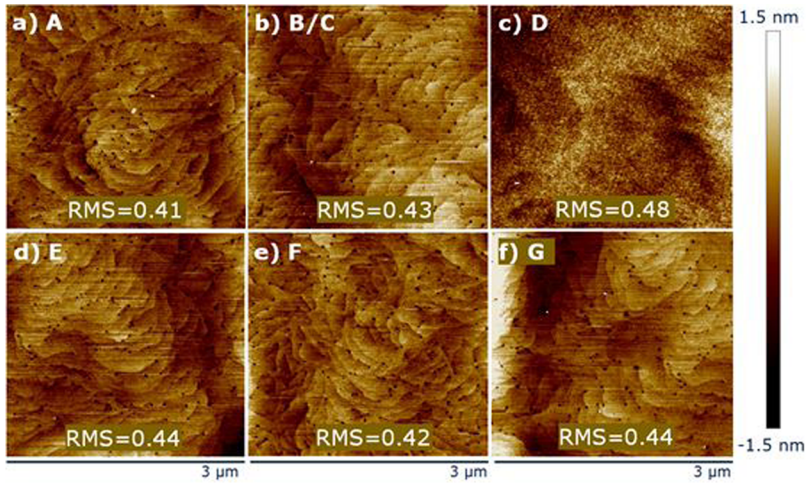

Figure 1. 3 μm × 3 μm AFM images and roughness RMS values of AlGaN surfaces after all processes A−G. The dark spots represent threading dislocations and are not etched by any processing but D: the roughness is slightly increased, and the typical surface terraces[15] are not observed anymore. For samples A−C and E−G, the surface morphology strongly depends on growth parameters and position of AFM needle rather than process related changes.

of Al_2O_3 at the surface which shows increased interaction with the polar water droplets leading to greater wettability.

In this paper, we investigate surface termination modifications by sessile drop measurements and find that the increase in surface energy is directly linked to the Φ_{SB} of the surface. Discussed surface modifications are all superficial and concern only the top surface atomic layers of the semiconductor. We provide an explanation why previously found surface oxidation[12] improves the Φ_{SB}. Furthermore, we show that the highest barrier is obtained by terminating the surface with the most electronegative atom, fluorine, as pictured in Scheme 1. Increasing the electronegativity difference between the metal and the adatom induces an increased dipole as it causes increased bond polarization. The increase of diiodomethane contact angles and detailed surface energy investigations support the presence of dipoles at the surface: due to the polarization, the apolar dispersion forces decrease which is reflected in the contact angles and further in the potential barrier at the metal−semiconductor junction.

EXPERIMENTAL SECTION

The GaN (0001) and 20 nm $Al_{0.22}Ga_{0.78}N$ on GaN (0001) on Si (111) samples are grown following a metal−organic chemical vapor deposition process. After the growth, all samples are cleaned in aqueous 1% hydrochloric acid (HCl) at room temperature for 5 min, rinsed with deionized water (d.i. H_2O), dried in gaseous nitrogen (N_2) and stored in air until the analysis or processed further by one of the seven sequences summarized in Table 1. All samples are subsequently analyzed between 30 and 45 min after the preparation by Auger electron spectroscopy, atomic force microscopy, contact angle measurements, and current−voltage measurements.

Using Auger electron spectroscopy (AES) on a Physical Electronics PHI-4700 at 5000 eV and 2 nA surface atomic changes of the samples are compared. Atomic force microscopy (AFM) roughness measurements are performed on a Veeco NanoScope Dimension TM 3100 with OTEPA tips in noncontact mode using the NanoScope SPM V5

DOI: 10.1021/acsami.5b06918
ACS Appl. Mater. Interfaces 2015, 7, 23124−23131

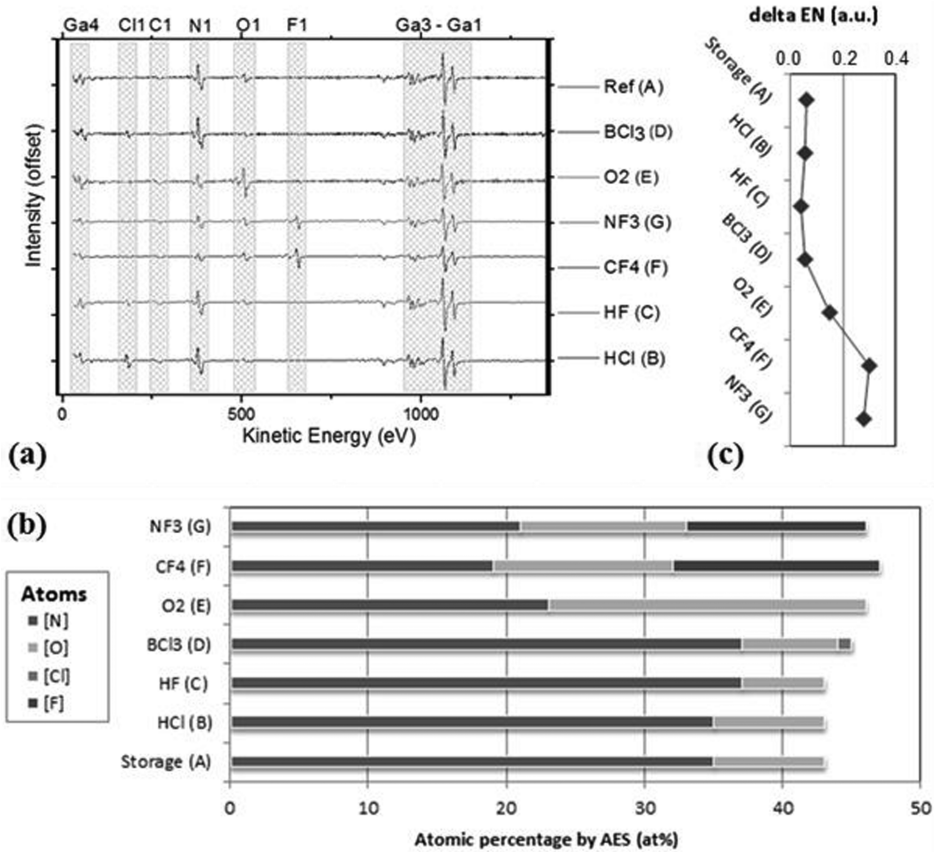

Figure 2. (a) AES spectra of GaN surfaces after processes A−G with accuracies between 85 and 90% for given measurement conditions. The chlorine peak after HCl clean corresponds to only 0.3%, after BCl_3 about 1% coverage. Carbon is systematically found on every sample but is not respected in the summarized (b) superficial anion concentrations (O, N, Cl, and F) as they are competing for the Ga bond. (c) Surface modifications lead to changes in surface-electronegativities and are compared to the theoretical Ga−N surface with $\chi_{Ga,N}$ = 5.42.

software for analysis. For each sample, process specific surface changes are investigated but none observed due to the general high inertness[13] of the material.

Values of the equilibrium contact angle (θ) are collected by applying the sessile drop method on a manual Ramé−Hart Contact Angle Goniometer at 21.4 ± 0.1 °C and 43.7% relative humidity. Three droplets per sample of distilled H_2O, diiodomethane (CH_2I_2), formamide ($HCONH_2$), and 2-methylpropan-1-ol (IBA; C_4H_9OH) are applied on the sample surface and measured after 15 s to ensure stability and reproducibility.[14] By varying the CH_2I_2 droplet sizes between 5 and 20 μL an absolute failure of 3.5° is observed; nevertheless, a sample to sample variation for constant droplet sizes of 10 μL of ±2° for $\theta \geq 10°$ and ±3° for $\theta < 10°$ is extracted, as with greater wettability, placing of the tangent is more critical.

Surface morphology and composition influence both, contact angle[16] as well as current−voltage (I−V) measurements.[17] Measurement conditions close to ideal surfaces have to be ensured to allow correct interpretation: the Al content is constant and GaN and AlGaN (0001) surfaces are known to be chemically inert and rigid.[18] AlGaN surfaces before and after processes A−G are shown in Figure 1. The roughness root-mean-square (RMS) values are extracted from these AFM images, varying between 0.44 ± 0.04 nm. Only process D changed the surface morphology by slightly etching the surface but did not show a significant increase in surface roughness. The same surface pattern is observed for GaN surfaces, where typical roughness values of 0.34 ± 0.03 nm are collected. In addition to being smooth,[15] a circular top view was seen for all droplets on each surface, proving chemical homogeneity.[17]

For I−V measurements, 100 nm Ni and 200 nm Au are evaporated on the AlGaN surface with a contact area of 1.96×10^{-3} cm^2. The evaporation through a noncontact shadow mask ensures surface stability after each surface treatment A−G. During deposition at 2.0×10^{-6} Torr the samples heat up to 70 ± 5 °C wherefore adsorbed water can evaporate. A Hewlett-Packard 4142B is used to measure I−V in the range from −10 to +5 V.

RESULTS

Figure 2a shows AES results after treatments A−G. As obtained from the AES data, none of the applied surface treatments influences the superficial Ga concentration of 42 ± 3 at%. The detectable N concentration varies between 18% and 37% as N is competing with the other electronegative atoms for the available Ga binding sites. The protruding inertness toward chemical surface modifications arises from the structural configuration: the gallium (Ga) atom shares three of its valence orbitals with three underlying nitrogen (N) atoms and only one Ga valence orbital is oriented toward the surface.[19] In combination with its electron configuration[20] this makes the Ga Lewis acidic, however the attack for Lewis bases is still rather difficult due to repulsion forces from the surrounding negatively charged N atom.[21] Electrochemical analysis[22] shows a high selectivity for anions to Ga with especially halogens being predicted to bind strongly to AlN or GaN surfaces.[23] Bermudez[24] showed for example that fluorine from XeF_2 plasma is found to cover GaN (0001) surfaces with 67% monolayer coverage by binding to the metal atom exclusively. Additionally, it is know that GaN (0001) surfaces terminate metal rich[25] and that the atomic charge at the surface is 0.691 for the Ga opposed to −1.382 for the N atom.[21] Other

DOI: 10.1021/acsami.5b06918
ACS Appl. Mater. Interfaces 2015, 7, 23124−23131

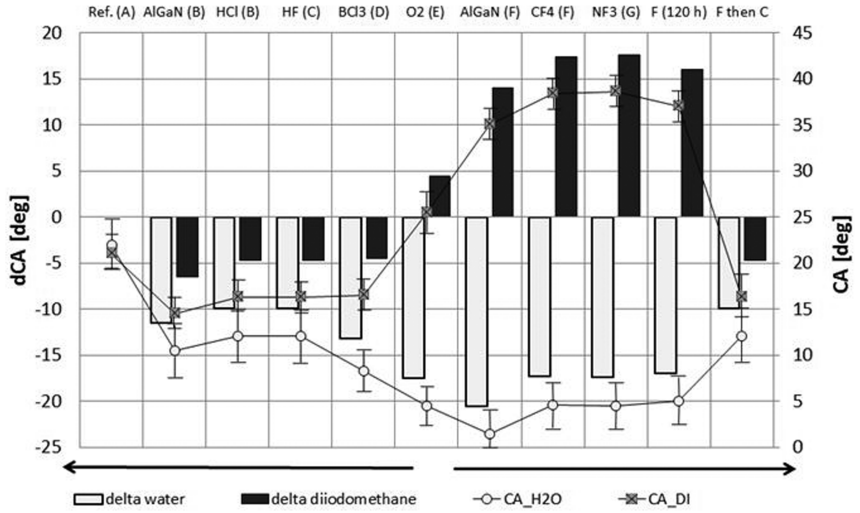

Figure 3. Equilibrium contact angles (CA) collected on GaN or AlGaN surfaces from diiodomethane and water at 21.4 °C after 15 s (scatter, right ordinate). The difference in averaged angles is plotted in the boxplot (left ordinate).

electronegative species should therefore substitute the N, hence the concentrations of negatively charged atoms can be added up to reach about 44 ± 2 at%.

From the AFM (Figure 1) no indication of material deposition or removal is seen which could influence the analysis. Chemical reactions are generally preferred at threading dislocations, grain boundaries,[26] or semipolar/nonpolar[27] planes rather than the (0001) surface, thus any reaction will show its influence in the form of the threading dislocations. Consequently, no surface etching can be seen for surfaces with treatments A−C and E−G. The chlorine from BCl_3/Cl_2 (D) does form a thermodynamically stable etch product with the group-XIII metal, such as $GaCl_3$(g) or GaCl(g), and $AlCl_3$(g) representing exothermic reactions and desorption of etch products for temperatures above 90 °C.[28,29] As a result the surface was slightly etched and the highest surface RMS of 0.48 nm was obtained. Nevertheless, due to the high chlorine affinity of the AlGaN surface, a residual 1% Cl remains at the surface. Additionally tested surface bromination results in a highly hygroscopic $GaBr_3$[30] termination which was too reactive in experimental conditions. In contrary, fluorine forms a stable Ga−F (or Al−F) bond with ΔH_f^0 = 577 kJ/mol or even 664 kJ/mol for Al−F[31] and desorption is suggested to occur only above T > 500 °C. From additional XPS analysis (not shown) no indication is found that O, Cl, or F is bound to N but exclusively to the metal atom, nor deposition of Teflon-like C−F surface species. A process sequence of CF_4 (or NF_3) plasma (G or H) followed by a wet clean (B or C) removes all superficial metal-F bonds and results in a surface as after only B or C measured by AES. Due to the substitution of superficial N atoms by other electronegative atoms namely fluoride, chloride, hydroxide, or oxide, a comparison of electronegativity differences between the surface terminations after process A−G is given in Figure 2c.

All anions competing for the available metal orbitals are influencing the surface dipoles. In surface-science approaches the Miedema[32] electronegativity of metals are often used to explain Φ_{SB} dependencies.[18] The electronegativity is important for the estimation of polarization especially if the created polarization is influencing present dipoles as we will discuss below. The Miedema electronegativities and their differences ($\Delta\chi$) of compounds ($\chi_{A,B} = (\chi_A \times \chi_B)^{1/2}$; $\chi_{Ga,N}$ = 5.42) is used to compare the modified surfaces to the ideal 50% Ga−N surface. They are calculated by summing up the atomic density of each Ga-anion pair (Figure 2b) and normalizing the resulting anion concentration to 100% as every anion is bound to a metal atom. We find that carbon is present on every surface between 6% and 12%. However, carbon is not taken into account for any calculation as it can bind to both, Ga and N.[33] A high relative surface electronegativity difference ($\Delta\chi$) is for instance induced by a high concentration of superficial Ga−F ($\chi_{Ga,F}$ = 6.11) bonds. The fluorine plasma treatment (F) covers up to 15% of the surface. Adding 12% Ga−O ($\chi_{Ga,O}$ = 5.72) and 19% Ga−N ($\chi_{Ga,N}$ = 5.42) and subsequently normalizing the 46% to 100% results in a relative surface electronegativity difference $\Delta\chi_{(F)}$ = +0.31 compared to the theoretical Ga−N surface. The wet chemical surface treatments B and C lead to the lowest oxygen concentrations, and highest amounts of Ga−N bonds; thus the lowest relative surface $\Delta\chi_{(C)}$ = +0.01 is achieved; see Figure 2c. The O_2 (E) process leads to the highest extend of Ga−O bonds and the third highest relative surface $\Delta\chi_{(E)}$ = +0.21. Although the BCl_3 plasma etches the surfaces slightly, some Ga−Cl ($\chi_{Ga,Cl}$ = 5.51) remains at the surface (1%) hence the relative surface $\Delta\chi_{(D)}$ = +0.12 is not much increased compared to A, B, or C. An increasing Al content will increase the $\Delta\chi$ because of its lower electronegativity compared to Ga; hence the size of the dipoles at the surface will increase which increases the interaction with polar solvents. The ideal $Al_{0.22}Ga_{0.78}N$ surface has a $\chi_{Al,Ga,N}$ = 5.37 and the same calculation is done by assuming the anions are statistically equally bound to metal.

The results of equilibrium θ values for H_2O and CH_2I_2 on GaN and AlGaN surfaces are collected in Figure 3. A generally high hydrophilicity of the surfaces is represented by θ_{H2O} of below 10°. Only the surface as received (A) and HCl and HF cleaned (B, C) reach θ_{H2O} above 10°. Especially the reference surface is probably influenced by adsorbents from the air, as the carbon concentration of 12% (A, reference after storage) is the highest of all samples, showing 6−8% for all other samples from the AES spectra. However, due to the increased relative error of applying a tangent at θ < 10°, the θ_{CH2I2} is the most significant for (Al)GaN investigations. It is the most sensitive to the relevant surface termination changes: the θ difference ($\Delta\theta$) after each process A−G in respect to A of the group-III-nitride surfaces is represented in Figure 3 (column). The exceptionally

DOI: 10.1021/acsami.5b06918
ACS Appl. Mater. Interfaces 2015, 7, 23124−23131

high θ_{CH2I2} after the fluorine plasma is surprisingly stable over time and easily reversed with an aqueous clean as no fluorine can be detected in AES afterward. Furthermore, the θ_{CH2I2} values return to 10−18°, thus the same as after any wet (aqueous) clean (B or C) only.

$\Delta\theta_{H2O}$ and $\Delta\theta_{CH2I2}$ generally follow opposed trends with exception of the sample A, because it is the most contaminated as discussed above. As expected, the AlGaN surfaces possess greater hydrophilicity compared to GaN due to a greater affinity of the aluminum toward oxygen; hence a higher amount of superficial Al−O bonds is present leading to an increased hydrogen bond interaction with water.[34] The strongly monopolar formamide also interacts with hydrogen bonds, although it is more sensitive to electron acceptors; additionally, its lower surface tension leads to a good wettability for all surfaces with $3° < \theta_{HCONH2} < 10°$ (not shown). The contact angle results reveal a dependence of the θ_{CH2I2} with the surface termination of GaN and AlGaN, as discussed below.

Figure 4 shows the Schottky barrier heights (Φ_{SB}) for the surfaces after processes A−G. They are calculated from $I-V$

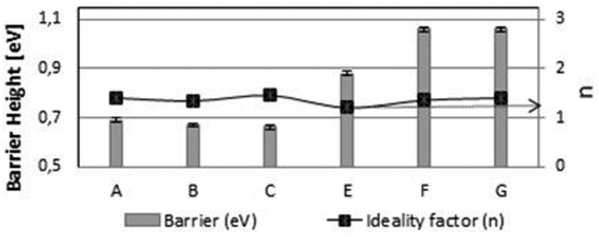

Figure 4. Extracted average Schottky barrier heights (left abscissa) of differently terminated surfaces after processes A−G; the BCl_3 (D) etches the surface wherefore the influences on the barrier height might not only be due to termination but also morphological changes. The ideality factor (n; right abscissa) varies between 1.1 and 1.5 for all samples.

data following the Richardson[6] approach, eqs 1 and 2. For the heterostructure samples, the product of Richardson constant (A_r = 24 A/cm^2 K^2) and the square of the temperature (T^2, T = 300 K) as well as Boltzmann constant (k) and the area of the Ni contact (A) are constant. The calculated Φ_{SB} correspond to zero electric field for the prepared Ni contacts on the AlGaN samples.

$$I = AA_rT^2\exp\left(-\frac{q\Phi_{SB}}{kT}\right)\exp\left[\left(\frac{qV}{nkT}\right) - 1\right] \quad (1)$$

$$n = \frac{q}{kT \times \text{slope}} \quad (2)$$

The Φ_{SB} increases from around 0.7 eV for the surfaces as received, cleans and samples with generally high surface N concentrations A to C to approximately 0.9 eV for lower surface N concentrations (E), and further to 1.1 eV for the fluorine plasma processes F and G (Figure 4). The ideality factor (n) lies between 1.1 and 1.5 for all calculated barrier heights. For the reason that the AlGaN surface was etched with the chlorine (D), we do not compare the Φ_{SB} with the other processes as a clear differentiation of surface morphological and termination influences cannot be ensured. The Al fraction (x) of $Al_xGa_{1-x}N$[35] as well as the surface morphology[13] are commonly discussed to have an influence on the barrier height. Nevertheless, the results show that a variation of Φ_{SB} for comparable surface morphologies and x = 22, depending on the surface termination is given. The highest Φ_{SB} is obtained after the fluorine termination. This mechanism is fundamentally different from the one observed after fluoride implantation into the AlGaN barrier,[36] where negative charges in the barrier are responsible to increase the potential within the barrier and thus reduce the leakage currents.

DISCUSSION

The atomistic investigation by AES of the surface on its own is not necessarily proving an increase in surface dipoles or polarization because the termination does not necessarily influence present potential barrier height solely by adsorbates. The direction of the established dipole has to increase or decrease the already present dipole to have an influence. Therefore, a more detailed analysis of surface energies by the sessile drop method is performed. Both, the contact angles and the barrier height, are seen to follow a trend with the surface termination. Only the sample as-received behaves slightly differently during sessile drop measurements compared to the trend seen by $I-V$ analysis (Figures 3 and 4): the resulting Φ_{SB} is comparable to the values collected after wet-cleaning of the (Al)GaN surfaces (B/C) whereas the contact angles are more comparable to the oxidized surfaces. We assume that this is due to unstable adsorbates at the surface, such as water, that evaporate before Ni deposition in given conditions. All other surface preparations are more stable against air and in experimental conditions; a more detailed analysis is given elsewhere.[37]

From the contact angle results, a trend of increasing θ_{CH2I2} with increasing $\Delta\chi$ can be derived. More detailed analysis reveals the surface energy components using the van Oss's model[38] (eq 3). The solid surface energy (γ_s) is divided into monopolar γ_s^+ and γ_s^- as well as apolar Lifshitz−van-der-Waals (γ_s^{LW}) components. Three solvents with known liquid surface energies ($\gamma_l^{\pm/LW}$) are needed for the evaluation, preferably of polar, monopolar, and apolar character.[38]

Table 2. Surface Energy γ Components by the van Oss Approach[38] after Processes A−G[a]

[mJ m^{-2}]	ref (A)	HCl (B)	HF (C)	BCl_3 (D)	O_2 (E)	CF_4 (F)	NF_3 (G)	AlGaN (B)	AlGaN (F)
γ_s^{LW}	47.5	48.8	48.8	48.8	46.0	40.4	40.4	44.0	42.0
γ_s^+	0.5	0.3	0.3	0.3	0.5	1.3	1.3	0.2	1.0
γ_s^-	46.9	53.2	53.2	54.2	55.5	54.7	54.7	53.6	55.2
γ_s^{AB}	9.2	7.4	7.4	7.5	10.1	16.6	16.6	7.2	14.7
γ_s^{Ges}	56.7	56.1	56.2	56.3	56.1	57.0	57.0	51.2	56.7

[a]With decreasing Lifshitz−van-der-Waals (LW) components, the acid−base (AB) component increases. Sample A has the highest carbon and increased oxygen at the surface. The main influences arise from the interaction with formamide and water. Two AlGaN surfaces, after clean (B) and fluorine (F) are given as examples.

DOI: 10.1021/acsami.5b06918
ACS Appl. Mater. Interfaces 2015, 7, 23124−23131

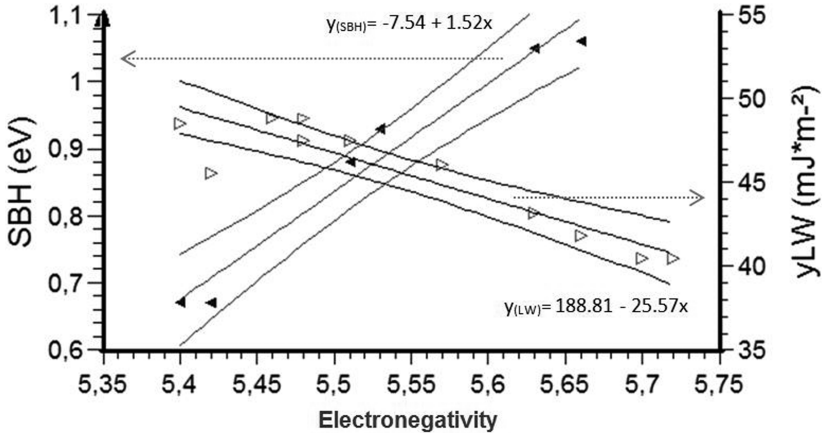

Figure 5. Correlation plot of the AlGaN and GaN surface electronegativity with the Schottky barrier height (SBH) and Lifschitz−van-der-Waals-component of surface energy in a 95% confidence interval. The surface energy values from Table 2 are extended by values for AlGaN surfaces after all processes A−G. For an additional Φ_{SB} value an AlGaN termination with 10% O, 9% F, and 24% N is added to get a medium χ value of 5.57. The correlation coefficients C are $C(\Phi) = 0.939$ with $\sigma = 0.17$ and $C(\gamma^{LW}) = 0.851$ with $\sigma = 3.35$.

$$\gamma_l(1 + \cos\theta) = 2\left(\sqrt{\gamma_s^{LW}\gamma_l^{LW}} + \sqrt{\gamma_s^{+}\gamma_l^{-}} + \sqrt{\gamma_s^{-}\gamma_l^{+}}\right) \quad (3)$$

From Table 2, a clear trend is seen of increasing surface energy values with both, increasing O and increasing halogen concentrations as given in Figure 2. Additionally, it emerges that the apolar Lifshitz−van-der-Waals components are dominant over polar interactions. Because the Ga−N surface itself is a very polar surface with an ionic character of the covalent bond of about 70%[39] the high Lifshitz−van-der-Waals component can be attributed to the polarizable surface termination which is susceptive to dispersion forces. During the adsorption process the dispersion is high if the molecules or atoms show a greater interaction with the surface than among each other. A dominant relative Lewis base polarity (γ_s^-) is found for all (Al)GaN surfaces, indicating that the surface is exclusively an electron donor. This monopolar surface behavior may be the result of intrinsic polarization fields and can explain why (Al)GaN (0001) surfaces cannot easily be wet-etched as it is commonly observed:[40] as the surface repels nucleophiles, a charge compensation by cations is needed. Such a mechanism is explained in ref.[41] Due to the fact that the surface terminates metal-rich,[42] Lewis acids will not attack the (Al)GaN surface easily neither. Additionally, the high polar behavior is the explanation why the monopolar solvents such as water and formamide wetten all samples similarly: they interact with the polar (Al)GaN surface.

From both, the θ_{CH2I2} (Figure 3) and Φ_{SB} (Figure 4) results it is clear that the F plasma treatments (F,G) show a significantly different feature than all other samples. The explanation is given in the surface energy components: The fluorine termination slightly lowers the monopolarity by increasing $\gamma_{(F)}^{+}$ to 1.3 mJ/m^2; but more importantly, γ_s^- increases from 47 to 55 mJ/m^2. Therefore, an increase in surface polarity is seen that arises from the more electronegative termination. This polarization is very stable because anions with equal negative charge are less polarizable the higher the electronegativity of the respective atoms. The increase in polarization is measured by $I-V$ because the potential barrier for electrons increases accordingly. Moreover, the decrease of γ_s^{LW} by approximately 8 mJ/m^2 over $\Delta\chi$ affirms the lowered polarization potential. Both, the increase of polar and decrease of dispersion forces lead to the increased wettability of water and decreased interaction with the apolar diiodomethane. As the θ_{CH2I2} further increases from 14° to 35° for GaN surfaces with increasing dipole momentum and decreasing polarizability between Ga−N < Ga−Cl < Ga−O < Ga−F, the θ_{CH2I2} are suggested to be most sensitive for investigations of (Al)GaN surface terminations.

Figure 5 correlates the γ_s^{LW} of the surface energy with $\Delta\chi$ supporting the discussed trend of decreasing apolar interaction. Furthermore, the adatom electronegativity of the surface termination is seen to have a strong dependence on the Φ_{SB}; the correlation with the $\Delta\chi$ is also given in Figure 5 (left abscissa).

The increase of ionicity of the covalent bond is dependent on the electronegativity of the adatom, following Pauling[6] and his proposal of partially ionized covalent bonds. The adatom electronegativity increases the polarization energy of the semiconductor surface due to a greater gap between the highest occupied and the lowest unoccupied orbital.[43] This increased ionization energy is responsible for the adatom-induced surface dipole shift in electronic charge[17] to the potential barrier. Most commonly, electronegativities of metals are correlated to the barrier height.[6] Our results show that the exchange of superficial nitrogen to anions with higher electronegativity, such as fluoride, hydroxide (oxide) or chloride, significantly increases experimentally obtained Φ_{SB} values. Therefore, it becomes clear how previously found surface anneal[12] improves the Φ_{SB} when increasing the amount and value of interfacial dipoles. The increase of Schottky diode characteristics including the barrier height, which is seen after the tetramethylammonium hydroxide,[13] is however more likely to be related to the smoothening of the GaN surfaces rather than the oxide removal.

A similar dependence on adatoms has been shown on GaAs (110) by the highly electronegative Cl and very low electronegative Cs adatoms on the surfaces finding an adatom dependent wave function tailoring into the semiconductor bandgap.[41] We suggest an even more sensitive correlation between Φ_{SB} and adatoms with anion character, thus a strong dependence on the dipole strength as well as concentration of adatoms. The refined and systematic increase of adatoms concentrations with increasing electronegativity is accomplished with surface treatments A−G. Fluorine, as the most electronegative atom, consequently leads to the greatest surface

DOI: 10.1021/acsami.5b06918
ACS Appl. Mater. Interfaces 2015, 7, 23124−23131

induced dipoles, hence the highest shift in the dipole charge within the adatom−substrate bonds and thus the highest potential barrier. Moreover, the barrier height might improve further if a (1 × 1) reconstruction with a complete monolayer of fluorine is achieved. Given correlation with the diiodomethane contact angles enables a cheap and fast method to evaluate and estimate Schottky barrier behavior.

CONCLUSION

The results show that for comparable AlGaN surfaces and metal work function, a significantly improved Schottky barrier height due to increased amounts of electronegative surface adatoms is achieved. Due to increasing anion electronegativity from N over O to F the adsorbate-induced surface dipole increases with increasing concentration of the latter. The established dipole leads to a band bending and an increased barrier height is measured. Choosing the most electronegative atom, fluorine, an improvement of Schottky barrier height from 0.7 to 1.1 eV could be achieved. The dipole changes are established by contact angle measurements: due to the higher polarization potential of anions with the same negative charge with increasing electronegativity, the Lifshitz−van-der-Waals component decreases at the same time as the polar surface energy component increases. Therefore, a more polarized nonetheless more stable dipole is created at the surface. Especially solvents with higher dispersion forces such as diiodomethane respond sensitively to such surface modifications with contact angles increasing from 14° for high nitride rich up to 39° for fluoride-rich surface terminations.

AUTHOR INFORMATION

Corresponding Author

*E-mail address: maria.reiner@infineon.com.

Notes

The authors declare no competing financial interest.

ACKNOWLEDGMENTS

We want to thank Prof. A. Marmur from the Faculty of Chemical Engineering at the Technion−Israel Institute of Technology as well as Prof. V. Ribitsch from the Institute of Chemistry at the University of Graz for their valuable discussion on the method.

REFERENCES

(1) Burk, A. A., Jr.; O'Loughlin, M. J.; Siergiej, R. R.; Agarwal, A. K.; Sriram, S.; Clarke, R. C.; MacMillan, M. F.; Balakrishna, V.; Brandt, C. D. SiC and GaN Wide Bandgap Semiconductor Materials and Devices. *Solid-State Electron.* **1999**, *43*, 1459−1464.

(2) Polyakov, A. Y.; Smirnov, N. B.; Govorkov, A. V.; Markov, A. V.; Yugova, T. G.; Dabiran, A. M.; Wowchak, A. M.; Cui, B.; Osinsky, A. V.; Chow, P. P.; Pearton, S. J.; Scherbatchev, K. D.; Bublik, V. T. Electrical and Structural Properties of AlN/GaN and AlGaN/GaN Heterojunctions. *J. Appl. Phys.* **2008**, *104*, 053702-1−053702-6.

(3) Sze, S. M. *Physics of Semiconductor Devices*, 2nd ed; John Wiley and Sons: NJ, 1981; pp 245−261.

(4) Tung, R. T. Recent Advances in Schottky Barrier Concepts. *Mater. Sci. Eng., R* **2001**, *35*, 1−138.

(5) Lee, C. T.; Lin, C. C.; Lee, H. Y.; Chen, P. S. Changes in Surface State Density due to Chlorine Treatment in GaN Schottky Ultraviolet Photodetectors. *J. Appl. Phys.* **2008**, *103*, 094504-1−094504-4.

(6) Tung, R. T. The Physics and Chemistry of the Schottky Barrier Height. *Appl. Phys. Rev.* **2014**, *1*, 011304-1−011304-54.

(7) Liu, Q. Z.; Lau, S. S. A Review of the Metal-GaN Contact Technology. *Solid-State Electron.* **1998**, *42*, 677−691.

(8) Kampen, T. U.; Mönch, W. Barrier Height of GaN Schottky Contacts. *Appl. Surf. Sci.* **1997**, *117/118*, 388−393.

(9) Marmur, A. Soft Contact: Measurement and Interpretation of Contact Angles. *Soft Matter* **2006**, *2*, 12−17.

(10) Fowkes, F. Additivity of Intermolecular Forces at Interfaces. *J. Phys. Chem.* **1963**, *67*, 2538−2541.

(11) Eickhoff, M.; Neuberger, R.; Steinhoff, G.; Ambacher, O.; Mueller, G.; Stutzmann, M. Wetting Behaviour of GaN Surfaces with Ga- or N-Face Polarity. *Phys. Status Solidi B* **2001**, *228*, 519−522.

(12) Shin, J.-H.; Park, J.; Jang, S. Y.; Jang, T.; Kim, K. S. Metal Induced Inhomogeneous Schottky Barrier Height in AlGaN/GaN Schottky Diodes. *Appl. Phys. Lett.* **2013**, *102*, 243505-1−243505-3.

(13) Zhuang, D.; Edgar, J. H. Wet Etching of GaN, AlN, and SiC: A Review. *Mater. Sci. Eng., R* **2005**, *48*, 1−46.

(14) Ghasemi, H.; Ward, C. A. Sessile-Water-Droplet Contact Angle Dependence on Adsorption at the Solid−Liquid Interface. *J. Phys. Chem. C* **2010**, *114*, 5088−5100.

(15) Tarsa, E. J.; Heying, B.; Wu, X. H.; Fini, P.; DenBaars, S. P.; Speck, J. S. Homoepitaxial Growth of GaN under Ga-stable and N-stable Conditions by Plasma-Assisted Molecular Beam Epitaxy. *J. Appl. Phys.* **1997**, *82*, 5472.

(16) Marmur, A.; Valal, D. Correlating Interfacial Tensions with Surface Tensions: A Gibbsian Approach. *Langmuir* **2010**, *26*, 5568−5575.

(17) Mönch, W. On the Physics of Metal-Semiconductor Interfaces. *Rep. Prog. Phys.* **1990**, *53*, 221−278.

(18) Polian, A.; Grimsditch, M.; Grzegory, I. Elastic Constants of Gallium Nitride. *J. Appl. Phys.* **1996**, *79*, 3343.

(19) Neugebauer, J.; Van de Walle, C. G. Atomic Geometry and Electronic Structure of Native Defects in GaN. *Phys. Rev. B: Condens. Matter Mater. Phys.* **1994**, *50*, 8067.

(20) Costales, A.; Kandalam, A. K.; Pendas, A. M.; Blanco, M. A.; Recio, J. M.; Pandey, R. First Principles Study of Polyatomic Clusters of AlN, GaN, and InN. 2. Chemical Bonding. *J. Phys. Chem. B* **2004**, *104*, 4368−4374.

(21) Mikroulis, S.; Georgakilas, A.; Kostopoulos, A.; Cimalla, V.; Dimakis, E.; Komninou, Ph. Control of the Polarity of Molecular-Beam-Epitaxy-Grown GaN Thin Films by the Surface Nitridation of Al_2O_3(0001) Substrates. *Appl. Phys. Lett.* **2002**, *80*, 2886.

(22) Chaniotakis, N. A.; Alifragis, Y.; Konstantinidis, G.; Georgakilas, A. Gallium Nitride-Based Potentiometric Anion Sensor. *Anal. Chem.* **2004**, *76*, 5552−5556.

(23) King, S. W.; Barnak, J. P.; Bremser, M. D.; Tracy, K. M.; Ronning, C.; Davis, R. F.; Nemanich, R. J. Cleaning of AlN and GaN Surfaces. *J. Appl. Phys.* **1998**, *84*, 5248−5260.

(24) Bermudez, V. M. Investigation of the Initial Chemisorption and Reaction of Fluorine (XeF_2) with the GaN(0001)-(1 × 1) Surface. *Appl. Surf. Sci.* **1997**, *119*, 147−159.

(25) Smith, A. R.; Feenstra, R. M.; Greve, D. W.; Neugebauer, J.; Northrup, J. E. Reconstructions of the GaN (0001) Surface. *Phys. Rev. Lett.* **1997**, *79*, 3934.

(26) Reiner, M.; Koller, Ch.; Pekoll, K.; Pietschnig, R.; Ostermaier, C. Relevance of Threading Dislocations for the Thermal Oxidation of GaN (0001). *MRS Online Proc. Libr.* **2015**, *1792*, 557−563.

(27) Jung, S.; Song, K. R.; Lee, S. N.; Kim, H. Wet Chemical Etching of Semipolar GaN Planes to obtain Brighter and Cost-Competitive Light Emitters. *Adv. Mater.* **2013**, *25*, 4470−4476.

(28) Bernard, C.; Chatillon, C.; Ait-Hou, A.; Hillel, R.; Monteil, Y.; Bouix, J. Thermodynamics of (Gallium + Chlorine)(g) I. Vapour-pressure Measurements and Thermodynamic Stability of GaCl(g), $GaCl_2$(g), $GaCl_3$(g), Ga_2Cl_2(g), Ga_2Cl4(g), and Ga_2Cl_6(g). *J. Chem. Thermodyn.* **1988**, *20*, 129−141.

(29) Utke, I.; Moshkalev, S.; Russel, P. *Nanofabrication Using Focused Ion and Electron Beams: Principles and application*; Oxford University Press: New York, 2012; pp 120.

(30) Klemm, W.; Tilk, W. Beiträge zur Kenntnis der Verbindungen des Galliums und Indiums. V. Die Eigenschaften der Galliumtrihalogenide. *Z. Anorg. Allg. Chem.* **1932**, *207*, 161−174.

DOI: 10.1021/acsami.5b06918
ACS Appl. Mater. Interfaces 2015, 7, 23124−23131

(31) Darwent, B. deB. Bond Dissociation Energies in Simple Molecules. *Nat. Stand. Ref. Data Ser., Natl. Bur. Stand. (U.S.)*; 1970; Vol. *31*.
(32) Miedema, A. R.; de Châtel, P. F.; de Boer, F. R. Cohesion in Alloys — Fundamentals of a Semi-Empirical Model. *Physica B+C* **1980**, *100* (1), 1−28.
(33) Seager, C. H.; Wright, A. F.; Yu, J.; Götz, W. Role of Carbon in GaN. *J. Appl. Phys.* **2002**, *92*, 6553.
(34) Buchheim, C.; Kittler, G.; Cimalla, V.; Lebedev, V.; Fischer, M.; Krischok, S.; Yanev, V.; Himmerlich, M.; Ecke, G.; Schaefer, J. A.; Ambacher, O. Tuning of Surface Properties of AlGaN/GaN Sensors for Nanodroplets and Picodroplets. *IEEE Sens. J.* **2006**, *6*, 881−886.
(35) Bradley, S. T.; Goss, S. H.; Hwang, J.; Schaff, W. J.; Brillson, L. J. Surface Cleaning and Annealing Effects on Ni/AlGaN Interface Atomic Composition and Schottky Barrier Height. *Appl. Phys. Lett.* **2004**, *85*, 1368−1370.
(36) Huang, S.; Chen, H.; Chen, K. J. Effects of the Fluorine Plasma Treatment on the Surface Potential and Schottky Barreir Height of $Al_xGa_{1-x}N$/GaN Heterostructures. *Appl. Phys. Lett.* **2010**, *96*, 233510.
(37) Reiner, M.; Lagger, P.; Schmid, M.; Frischmuth, T.; Stadtmueller, M.; Schmid, U.; Pietschnig, R.; Ostermaier, C., manuscript in preparation.
(38) Van Oss, C. J.; Chaudhury, M. K.; Good, R. J. Interfacial Lifshitz-van der Waals and Polar Interactions in Macroscopic systems. *Chem. Rev.* **1988**, *88*, 927−941.
(39) Pearton, S. J. *Processing of Wide-Bandgap Semiconductors*; Noyes Publications: New York, 2000; pp 81.
(40) Vartuli, C. B.; Pearton, S. J.; Abernathy, C. R.; MacKenzie, J. D.; Ren, F.; et al. Wet Chemical Etching Survey of III-Nitrides. *Solid-State Electron.* **1997**, *41*, 1947−1951.
(41) Zhuang, D.; Edgar, J. H. Wet Etching of GaN, AlN and SiC: A Review. *Mater. Sci. Eng., R* **2005**, *48*, 1−46.
(42) Smith, A.R.; Feenstra, R. M.; Greve, D. W.; Shin, M.-S.; Skowronski, M.; Neugebauer, J.; Northrup, J. E. Reconstructions of GaN(0001) and (000−1) Surfaces: Ga-rich Metallic Structures. *J. Vac. Sci. Technol., B: Microelectron. Process. Phenom.* **1998**, *16*, 2242−2259.
(43) Lebedev, M. V. Surface Modification of III−V Semiconductors: Chemical Processes and Electronic Properties. *Prog. Surf. Sci.* **2002**, *70*, 153−186.

DOI: 10.1021/acsami.5b06918
ACS Appl. Mater. Interfaces 2015, 7, 23124−23131